Title: Halogen bonding to the azulene π-system: cocrystal design of pleochroism

Authors: Jogirdas Vainauskas, Filip Topić, Oleksandr S. Bushuyev, Christoper J. Barrett*, Tomislav Friščić*

Abstract: We describe the rational development a design to create pleochroic molecular solids, by using C−I···π halogen bonds to pre-organise different types of chromophores in a cocrystal. Using as a blueprint the structure of a non-dichroic naphthalene cocrystal, we show how the systematic introduction of chromophores able to act as halogen bond donors or acceptors enables the construction of optically interesting dichroic or pleochroic solids, demonstrating the reliability of C−I···π halogen bonds in designing new properties.

Main text: Self-assembly through strong and/or directional interactions such as hydrogen or halogen bonds (XBs) in the solid state is a powerful approach to access materials that interact with light in a controllable, pre-designed manner, such as photo-reactive or photo-mechanical solids.[1,2] We have previously demonstrated a cocrystallisation strategy to create dichroic materials, whose appearance switches between coloured and colourless when rotated in plane-polarised light, due to different light absorption depending on the orientation of its polarisation.[3] The strategy is based on accomplishing parallel alignment of chromophores, and thus their transition dipole moments, throughout the crystal.[‡] Such alignment yields crystals exhibiting dichroism independent of the face being observed. This design for dichroic solids relied on using cocrystal formers (coformers) capable of forming strong XBs of I···N type to direct parallel alignment of azobenzene (azo) chromophores within linear supramolecular chains.

Here, we show a strategy to design not only dichroic, but also pleochroic molecular crystals (Fig. 1a), *i.e.* solids that exhibit different colours depending on their orientation with respect to plane-polarised light.[3] The presented strategy is the first to design pleochroism in molecular solids and is based on XB to the π-system of azulene (**azu**, Fig. 1b), representing a rare example of deliberate use of I···π interactions[4–6] for the predictable assembly of a functional structure, and the first report of **azu**[7,8] as a structural and functional (chromophoric) building block in crystal engineering.

Our design was inspired by the reported structure of a cocrystal of 1,4-diiodotetrafluorobenzene (**14tfib**, Fig. 1b) with naphthalene (**nap**) (CSD NICTAW).[5] The cocrystal (**nap**)(**14tfib**)$_2$ is composed of ladder-like tapes held by XBs between pairs of parallel **14tfib** molecules (rails) acting as donors, associated with **nap** molecules (rungs) as π-based acceptors. The chains assemble in a parallel fashion, giving rise to a structure in which all **14tfib** and all **nap** molecules, respectively, are mutually parallel. While (**nap**)(**14tfib**)$_2$ is colourless and not dichroic (see ESI), we speculated that replacing **nap** with isomeric, coloured **azu** could yield an isostructural system that would exhibit dichroism due to parallel alignment of **azu** chromophores. Notably, **azu** is blue in colour due to a weak absorption in the visible spectrum associated with the $S_0 \rightarrow S_1$ transition.[7,9] Recrystallisation from a solution containing **azu** and **14tfib** in the 1:2 stoichiometric ratio yielded two types of blue crystals, with either prismatic (from hexane) or plate-like (from acetone) morphologies. Single crystal X-ray diffraction on the plate-like crystals revealed the formation of XB chains of alternating **14tfib** and **azu** molecules (Fig. 2a). Here, **azu** molecules are periodically bridged either by a single molecule or a pair of stacked molecules of **14tfib**, giving rise to the composition (**azu**)$_2$(**14tfib**)$_3$. Each **azu** molecule is ordered and participates in XB in a non-symmetrical way: on one face each **azu** molecule engages both the

5- and the 7-membered rings in XB formation (distances between the iodine atom and the mean plane of **azu** $d_{I\cdots plane}$ of 3.29 and 3.43 Å, respectively), while on the other **azu** face XBs form only *via* the five-membered ring ($d_{I\cdots plane}$ = 3.32 Å). All these distances are considerably shorter than the sum of the van der Waals radii (3.68 Å), indicating XB formation.[10]

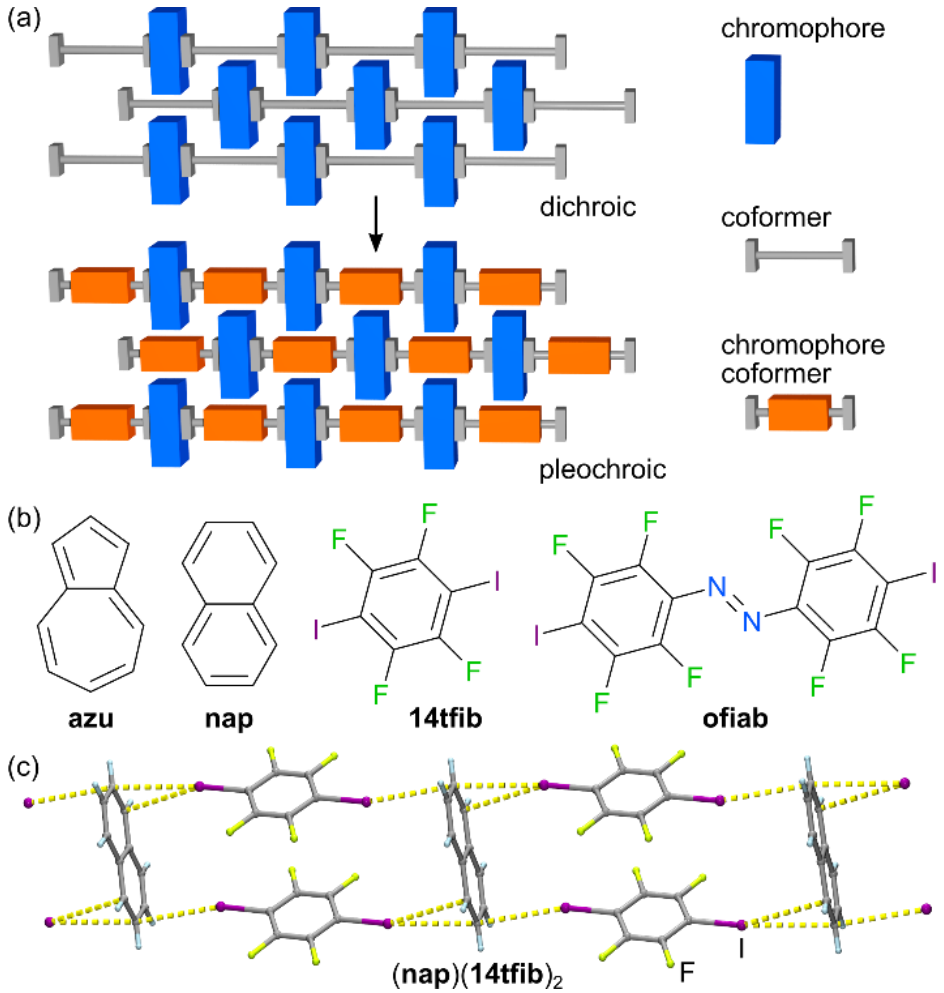

Figure 1. (a) Chromophore motifs exhibiting dichroism or pleochroism. (b) Molecular structures of **azu**, **nap**, **14tfib** and **ofiab**. (c) Ladder-like structure of (**nap**)(**14tfib**)$_2$, as seen perpendicular to the plane (101).

X-ray analysis of the prismatic crystals revealed a structure analogous to (**nap**)(**14tfib**)$_2$, but with **azu** as the rungs of the XB ladder, disordered over crystallographic centres of symmetry. Disorder means that each iodine atom in a **14tfib** molecule can be associated with either the 5- or the 7-membered ring of a neighbouring **azu**, giving rise to a range of I···C distances (3.38(2)–3.54(2) Å) and two distinct distances between iodine atoms and the mean plane of **azu** (3.345 and 3.411 Å).

Molecular crystals based on **azu** are very rare, with the Cambridge Structural Database (CSD) containing structures for not more than 12 solids, of which only two are cocrystals (CSD codes AZUNBZ/AZUNBZ01 and QEMKOJ), both based on aromatic ring stacking.[11,12] CSD search also revealed that, unless coordinated to a metal, **azu** molecules are not disordered in only two structures (CSD codes LAKFIN, QEMKOJ).[12,13] Thus, while (**azu**)(**14tfib**)$_2$ and

(**azu**)$_2$(**14tfib**)$_3$ represent unique cases of XB cocrystals based on this arene, (**azu**)$_2$(**14tfib**)$_3$ is a rare example of an ordered, non-covalently bound **azu** in a crystal.

As **azu** molecules in both (**azu**)(**14tfib**)$_2$ and (**azu**)$_2$(**14tfib**)$_3$ (Fig. 2c) are aligned in parallel, the crystals are anticipated to be dichroic. This is confirmed by colour changes upon rotating the crystals under plane-polarised light (Fig. 2). Crystals of (**azu**)$_2$(**14tfib**)$_3$ appear dark blue in one orientation, and almost colourless when rotated in the plane by 90^o (Fig. 2b), while (**azu**)(**14tfib**)$_2$ transitions from deep to light blue (Fig. 2e).

The cocrystal (**azu**)(**14tfib**)$_2$ is isostructural to (**nap**)(**14tfib**)$_2$, while the structure of (**azu**)$_2$(**14tfib**)$_3$ can be related to that of (**azu**)(**14tfib**)$_2$ by removing 25 % of **14tfib** molecules. These observations indicate that the I···π chain motif is sufficiently robust to withstand both the replacement of **nap** with its isomer **azu**, as well as changes to the cocrystal composition. Consequently, we were encouraged to replace the colourless **14tfib** coformer with the red azobenzene (azo) dye *trans*-4,4'-octafluorodiiodoazobenzene (**ofiab**). Such a change would effectively replace the **14tfib** rails with another chromophore. The expected structure would be pleochroic due to the two different types of chromophores, blue **azu** and orange-red **ofiab**, being organised in a mutually perpendicular fashion.

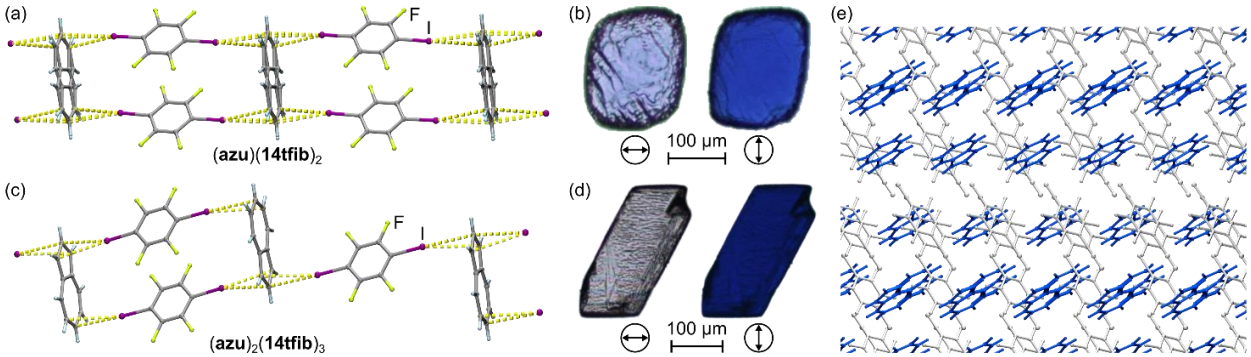

Figure 2. (a) Ladder-like structure of (**azu**)(**14tfib**)$_2$ view approx. perpendicular to the plane (101). (b) Dichroism of (**azu**)(**14tfib**)$_2$, face (001). (c) Crystal structure of (**azu**)$_2$(**14tfib**)$_3$, view approx. perpendicular to the plane (110), showing the ordering of **azu** and the (**azu**)$_2$(**14tfib**)$_2$ moieties bridged by **14tfib**. (d) Dichroism of (**azu**)$_2$(**14tfib**)$_3$, face (110). (e) Mutually parallel **azu** molecules in the structure of (**azu**)$_2$(**14tfib**)$_3$, with **azu** and **14tfib** shown in blue and light grey, respectively.

Crystallisation from a solution containing **azu** and **ofiab** in a 1:2 stoichiometric ratio produced elongated crystals. Crystal structure analysis revealed the composition (**azu**)(**ofiab**)$_2$ and a structure composed of anticipated I···π XB ladders with **ofiab** rails and **azu** rungs (Fig. 3a). Like in the analogous (**azu**)(**14tfib**)$_2$, the **azu** units in (**azu**)(**ofiab**)$_2$ are disordered over two coplanar positions around centres of symmetry. As the **azu** and **ofiab** chromophores are mutually roughly perpendicular in this structure (mean planes at an angle of 86.62°), the crystals are expected to exhibit pleochroism in plane-polarised light. Indeed, when observed with the polarised light microscope the crystals were found to change colour upon rotation, from red caused by **ofiab**, to blue caused by **azu** (Fig. 3b).

Exploring different stoichiometric compositions during the cocrystallisation of **azu** with **ofiab** led to the observation of another cocrystal form, (**azu**)$_3$(**ofiab**)$_2$. While the stoichiometric composition of this cocrystal is different than any observed in case of **azu** and **14tfib**, the structure still exhibits I···π XBs between components (Fig. 3c). Here, however, XBs lead to discrete

(**azu**)$_2$(**ofiab**)$_2$ assemblies separated by additional **azu** molecules that are disordered around centres of symmetry. The (**azu**)$_2$(**ofiab**)$_2$ assemblies throughout the cocrystal are all organised in parallel, enabling both the parallel alignment of the chromophores of the same type, and roughly perpendicular alignment of **azu** and **ofiab** chromophores (mean planes at an angle of 82.06°). However, the additional **azu** molecules occupying the space between the XB assemblies are not parallel to those within the assemblies. This implies that the cocrystal might again exhibit pleochroic behaviour but, as all **azu** molecules in the structure are no longer mutually parallel, the absorption of **azu** will not be fully extinguished upon rotating the crystal in plane-polarised light. This is consistent with the observed behaviour, as rotating the cocrystal under plane-polarised light switches its colour from blue, due to absorption of only **azu**, to orange-brown, which can be associated with simultaneous absorption of **ofiab** and **azu** (Fig. 3d).

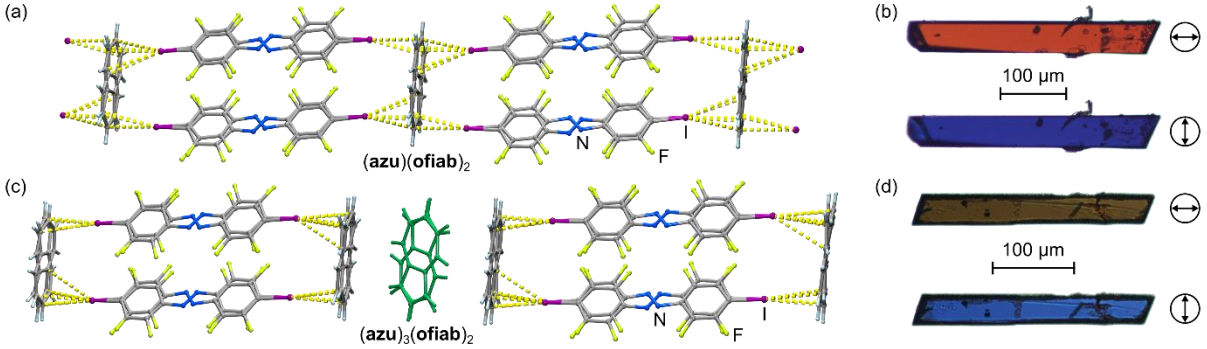

Figure 3. (a) Ladder-like structure of (**azu**)(**ofiab**)$_2$, view perpendicular to the plane (111). (b) Pleochroism of (**azu**)(**ofiab**)$_2$, face (001). (c) Structure of (**azu**)$_3$(**ofiab**)$_2$, comprising discrete (**azu**)$_2$(**ofiab**)$_2$ moieties and additional **azu** molecules (in green), view perpendicular to the plane (230). (d) Pleochroism of (**azu**)$_3$(**ofiab**)$_2$, face (001).

The observed crystal structures and optical properties confirm the utility of I···π XBs as a reliable design element in the synthesis of functional organic cocrystals. While cocrystals of **azu** with either **14tfib** or **ofiab** appear in at least two different stoichiometric compositions, all structures exhibit the I···π motif that aligns the **azu** perpendicularly to the π-system of the XB donor. The resilience of this XB motif to stoichiometric variation led us to explore the possibility of other cocrystal compositions by mechanochemical liquid-assisted grinding (LAG), previously noted for high cocrystal screening efficiency.[6,14] Mixtures of **azu** or **nap** with **14tfib** were milled in stoichiometric ratios 2:1, 1:1, 2:3 and 1:2, with addition of a small amount (50 µL) of nitromethane (liquid-to-solids ratio η = 0.25 µL/mg).[15] Milling was done in 14 mL stainless steel (**ss**) jars containing a pair of 0.7 g **ss** balls, using a Form-Tech Scientific FTS1000 mill operating at 1800 rpm (30 Hz). Powder X-ray diffraction (PXRD) patterns (Fig. 4) of the milled mixtures of **azu** and **14tfib** showed the formation of (**azu**)(**14tfib**)$_2$ only when the stoichiometric ratio of **azu** to **14tfib** was 1:2. Other compositions led to the formation of (**azu**)$_2$(**14tfib**)$_3$ alone or in mixture with **azu**. For mixtures of **nap** and **14tfib**, all explored compositions yielded (**nap**)(**14tfib**)$_2$, alone or in a mixture with **nap**. The mechanochemically prepared (**azu**)(**14tfib**)$_2$, (**azu**)$_2$(**14tfib**)$_3$ and (**nap**)(**14tfib**)$_2$ were analysed by infrared spectroscopy, as well as combined thermogravimetric analysis and differential scanning calorimetry (TGA/DSC), which revealed the melting points of the cocrystals to be 91.1, 90.0 and 88.1 °C, respectively (see ESI).

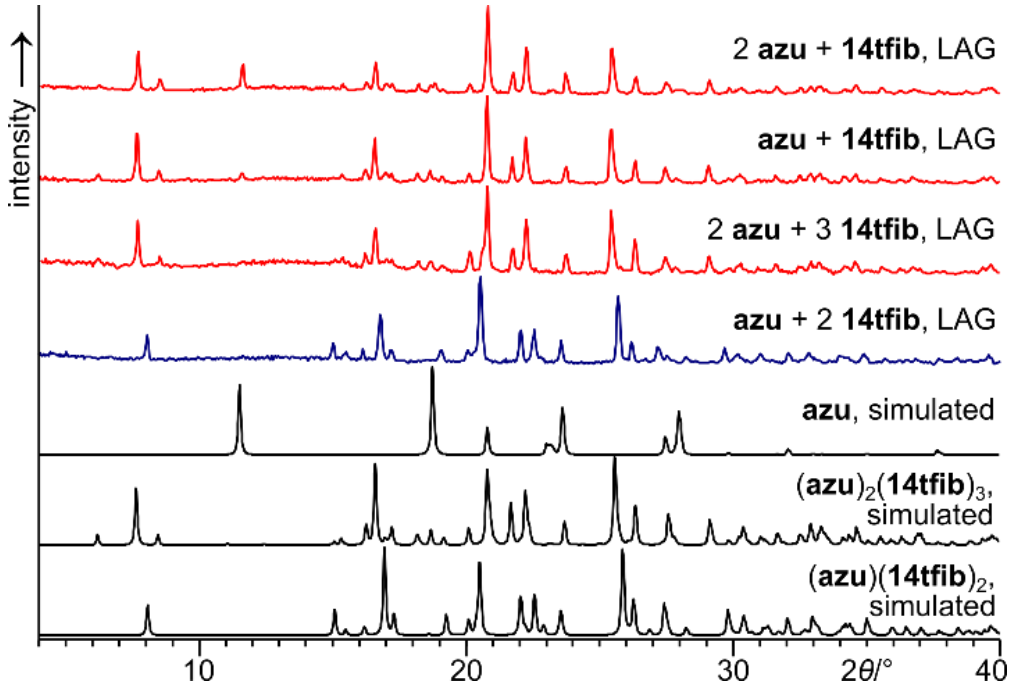

Figure 4. Comparison of PXRD patterns obtained in the cocrystallisation screening for **azu** and **14tfib** with the simulated patterns for **azu**, (**azu**)$_2$(**14tfib**)$_3$ and (**azu**)(**14tfib**)$_2$.

The results of mechanochemical screening suggest that the formation of the (**azu**)$_2$(**14tfib**)$_3$ phase is specific to **azu**, and that an analogous phase with **nap** is not accessible. This observation was investigated by periodic density functional theory (DFT) calculations in CASTEP[16] using the GGA-type PBE functional[17] in combination with MBD* semi-empirical dispersion correction,[18] previously shown successful in modelling XB cocrystals (see ESI).[19] Specifically, we calculated the formation energies (E_f) for the cocrystals of **azu** and **nap** with **14tfib**, as well as for the hypothetical (**nap**)$_2$(**14tfib**)$_3$ structure generated from (**azu**)$_2$(**14tfib**)$_3$ by replacing each **azu** with a **nap** moiety. The calculated E_f values for the observed cocrystals (**azu**)(**14tfib**)$_2$, (**nap**)(**14tfib**)$_2$ and (**azu**)$_2$(**14tfib**)$_3$ were all exothermic by −4.10, −1.32 and −5.00 kJ/mol, respectively. In contrast, the E_f for the hypothetical (**nap**)$_2$(**14tfib**)$_3$ was found to be at least +3.65 kJ/mol, consistent with the fact that it was not observed. We also investigated the importance of the unusual ordering of **azu** for the formation of (**azu**)$_2$(**14tfib**)$_3$, by optimising three different versions of this structure (Fig. 5b−d): the experimental one, *exp*-(**azu**)$_2$(**14tfib**)$_3$; one with the inverted orientation of all **azu** molecules, *inv*-(**azu**)$_2$(**14tfib**)$_3$; and an alternating model, *alt*-(**azu**)$_2$(**14tfib**)$_3$, in which every second molecule of **azu** along an XB chain is inverted with respect to the experimental structure. Compared to *exp*-(**azu**)$_2$(**14tfib**)$_3$, the *alt*- and *inv*-(**azu**)$_2$(**14tfib**)$_3$ models were found to be +4.25 and +9.28 kJ/mol higher in energy, respectively. Such energy differences can be considered as sufficient driving forces for the ordering of **azu** and are consistent with its asymmetric charge distribution, with the 5-membered ring more electron-rich than the 7-membered one and thus a better XB acceptor (Fig. 5a).

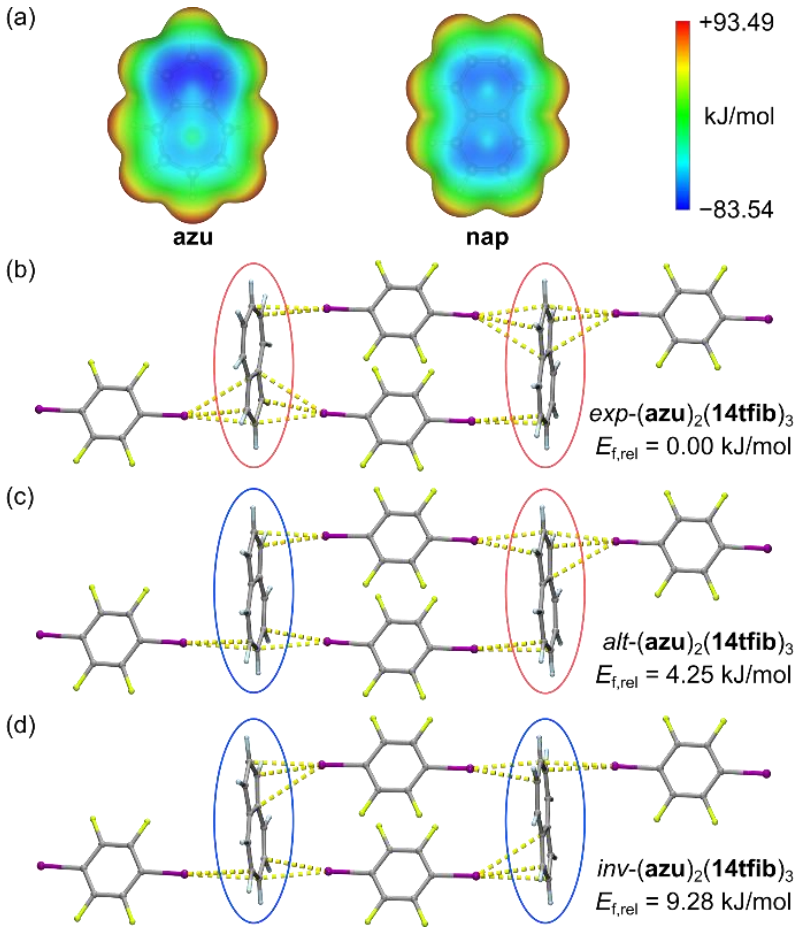

Figure 5. (a) Electrostatic potential surfaces of **azu** and **nap**. Structural models of (**azu**)$_2$(**14tfib**)$_3$ used in periodic DFT computations, and respective relative energies per formula unit: (b) experimental, *exp*-(**azu**)$_2$(**14tfib**)$_3$; (c) putative alternating, *alt*-(**azu**)$_2$(**14tfib**)$_3$; (d) putative inverted, *inv*-(**azu**)$_2$(**14tfib**)$_3$. Different orientations of the **azu** moieties are highlighted: experimentally observed (red) and the inverted (blue).

In conclusion, we demonstrated the use of robust I···π halogen bonds with a hydrocarbon acceptor as a means to accomplish the synthesis of dichroic and pleochroic molecular solids. To the best of our knowledge, this represents the first example of using I···π halogen bonds for the reliable formation of supramolecular architectures with predictable properties, introducing azulene as a robust π-based hydrocarbon XB acceptor. The robustness of XB interactions to azulene is illustrated by varying the type and stoichiometric ratio of cocrystal components without disrupting the overall XB chain architecture in 3 out of 4 cases, corresponding to a supramolecular yield of 75%.[20] We also highlight the importance of the asymmetric charge distribution in the azulene system which, through the ordering of the azulene moiety in the solid state, enabled the formation of an additional cocrystal composition not observed with naphthalene. The presented work represents a significant advance in developing optically functional and versatile molecular solids based on XB with π-acceptors, and we are now exploring the use of non-iodine XB donor systems.

Acknowledgments: We acknowledge the use of the supercomputers MP2 and Cedar, enabled by Calcul Québec and WestGrid, respectively, and Compute Canada. We acknowledge NSERC

Discovery (TF, CB) and Accelerator grants (TF), and for Vanier Graduate (OSB) and Banting Postdoctoral (FT) Fellowships.

Footnotes and references:

‡ In azobenzene the transition dipole moment is aligned with the longest molecular axis,[21] and for azulene with the shortest.[22]

1 (a) J.-C. Christopherson, F. Topić, C. J. Barrett, T. Friščić, *Cryst. Growth Des.*, 2018, **18**, 1245; (b) L. Sun, Y. Wang, F. Yang, X. Zhang, W. Hu, *Adv. Mater.*, 2019, **31**, 1902328; (c) Y. Huang, Z. Wang, Z. Chen, Q. Zhang, *Angew. Chem. Int. Ed.*, 2019, **58**, 9696.

2 (a) T. Caronna, R. Liantonio, T. A. Logothetis, P. Metrangolo, T. Pilati, G. Resnati, *J. Am. Chem. Soc.*, 2004, **126**, 4500; (b) B. Kahr, J. Freudenthal, S. Phillips and W. Kaminsky, *Science*, 2009, **324**, 1407; (c) P. Naumov, J. Kowalik, K. M. Solntsev, A. Baldridge, J.-S. Moon, C. Kranz, L. M. Tolbert, *J. Am. Chem. Soc.*, 2010, **132**, 5845; (d) O. S. Bushuyev, T. C. Corkery, C. J. Barrett, T. Friščić, *Chem. Sci.*, 2014, **5**, 3158; (e) M. A. Sinnwell, L. R. MacGillivray, *Angew. Chem. Int. Ed.*, 2016, **55**, 3477; (f) L. Zhu, R. O. Al-Kaysi, C. J. Bardeen, *Angew. Chem. Int. Ed.*, 2016, **55**, 7073; (g) A. Carletta, F. Spinelli, S. d'Agostino, B. Ventura, M. R. Chierotti, R. Gobetto, J. Wouters, F. Grepioni, *Chem. Eur. J.*, 2017, **23**, 5317; (h) P. Gupta, D. P. Karothu, E. Ahmed, P. Naumov, N. K. Nath, *Angew. Chem. Int. Ed.*, 2018, **57**, 8498.

3 (a) O. S. Bushuyev, T. Friščić and C. J. Barrett, *Cryst. Growth Des.*, 2016, **16**, 541; (b) J.-C. Christopherson, K. P. Potts, O. S. Bushuyev, F. Topić, I. Huskić, K. Rissanen, C. J. Barrett, T. Friščić, *Faraday Discuss.*, 2017, **46**, 6368.

4 H. Y. Gao, Q. J. Shen, X. R. Zhao, X. Q. Yan, X. Pang, W. J. Jin, *J. Mater. Chem.*, 2012, **22**, 5336.

5 Q. J. Shen, X. Pang, X. R. Zhao, H. Y. Gao, H.-L. Sun, W. J. Jin, *CrystEngComm*, 2012, **14**, 5027.

6 S. d'Agostino, F. Grepioni, D. Braga, B. Ventura, *Cryst. Growth Des.*, 2015, **15**, 2039.

7 H. Xin and X. Gao, *ChemPlusChem*, 2017, **82**, 945.

8 B. Dittrich, F. P. A. Fabbiani, J. Henn, M. U. Schmidt, P. Macchi, K. Meindl, M. A. Spackman, *Acta Cryst.*, 2018, **B74**, 416.

9 M. Murai, S.-Y. Ku, N. D. Treat, M. J. Robb, M. L. Chabinyc, C. J. Hawker, *Chem. Sci.*, 2014, **5**, 3753.

10 M. Mantina, A. C. Chamberlin, R. Valero, C. J. Cramer, D. G. Truhlar, *J. Phys. Chem. A*, 2009, **113**, 5806.

11 (a) A. W. Hanson, *Acta Cryst.*, 1965, **19**, 19; (b) D. S. Brown, S. C. Wallwork, *Acta. Cryst.*, 1965, **19**, 149.

12 I. A. Tikhonova, K. I. Tugashov, F. M. Dolgushin, A. A. Yakovenko, B. N. Strunin, P. V. Petrovskii, G. G. Furin, V. B. Shur, *Inorg. Chim. Acta*, 2006, **359**, 2728.

13 O. Ohmori, M. Kawano, M. Fujita, *Angew. Chem. Int. Ed.*, 2005, **44**, 1962.

14 S. Karki, T. Friščić, W. Jones, *CrystEngComm*, 2009, **11**, 470.

15 T. Friščić, S. L. Childs, S. A. A. Rizvi and W. Jones, *CrystEngComm*, 2009, **11**, 418.

16 S. J. Clark, M. D. Segall, C. J. Pickard, P. J. Hasnip, M. I. J. Probert, K. Refson, M. C. Payne, *Z. Kristallogr.*, 2005, **220**, 567.

17 J. P. Perdew, K. Burke and M. Ernzerhof, *Phys. Rev. Lett.*, 1996, **77**, 3865.

18 A. Ambrosetti, A. M. Reilly, R. A. DiStasio, A. Tkatchenko, *J. Chem. Phys.*, 2014, **140**, 18A508.
19 M. Arhangelskis, F. Topić, P. C. Hindle, R. Tran, A. J. Morris, D. Cinčić, T. Friščić, *Chem. Commun.*, DOI:10.1039/D0CC02935A.
20 C. B. Aakeröy, A. M. Beatty, B. A. Helfrich, *J. Am. Chem. Soc.*, 2002, **124**, 14425.
21 T. S. Yankova, N. A. Chumakova, D. A. Pomogailo, A. Kh. Vorobiev, *Liq. Cryst.*, 2013, **40**, 1135.
22 R. Pariser, *J. Chem. Phys.*, 1956, **25**, 1112.